NANO MICRO small

Centimeter-Scale High-Resolution Metrology of Entire CVD-Grown Graphene Sheets

Jennifer Reiber Kyle, Ali Guvenc, Wei Wang, Maziar Ghazinejad, Jian Lin, Shirui Guo, Cengiz S. Ozkan, and Mihrimah Ozkan**

***A** high-throughput metrology method for measuring the thickness and uniformity of entire large-area chemical vapor deposition-grown graphene sheets on arbitrary substrates is demonstrated. This method utilizes the quenching of fluorescence by graphene via resonant energy transfer to increase the visibility of graphene on a glass substrate. Fluorescence quenching is visualized by spin-coating a solution of polymer mixed with fluorescent dye onto the graphene then viewing the sample under a fluorescence microscope. A large-area fluorescence montage image of the dyed graphene sample is collected and processed to identify the graphene and indicate the graphene layer thickness throughout the entire graphene sample. Using this metrology method, the effect of different transfer techniques on the quality of the graphene sheet is studied. It is shown that small-area characterization is insufficient to truly evaluate the effect of the transfer technique on the graphene sample. The results indicate that introducing a drop of acetone or liquid poly(methyl methacrylate) (PMMA) on top of the transfer PMMA layer before soaking the graphene sample in acetone improves the quality of the graphene dramatically over immediately soaking the graphene in acetone. This work introduces a new method for graphene quantification that can quickly and easily identify graphene layers in a large area on arbitrary substrates. This metrology technique is well suited for many industrial applications due to its repeatability and flexibility.*

J. R. Kyle, A. Guvenc, Prof. M. Ozkan
Department of Electrical Engineering
University of California
Riverside , CA 92521, USA
E-mail: mihri@ee.ucr.edu
W. Wang, M. Ghazinejad, J. Lin, Prof. C. S. Ozkan
Department of Mechanical Engineering and the Materials Science and Engineering Program
University of California
Riverside, CA 92521, USA
E-mail: cengiz.ozkan@ucr.edu
S. Guo
Department of Chemistry
University of California
Riverside, CA 92521, USA

DOI: 10.1002/smll.201100263

1. Introduction

Graphene is a two-dimensional sheet of graphite consisting of one to ten layers of carbon atoms arranged in hexagonal lattices. Only six years after first fabricating graphene in the laboratory, Geim and Novoselov were awarded the Nobel Prize in physics for their work on graphene.[1] This relatively short time between discovery and recognition is due in part to the fact that graphene was extensively studied theoretically long before it was discovered experimentally. The greatest obstacle to experimental discovery of graphene was the difficulty in detecting the graphene sheets. A single-layer graphene sheet is only ≈0.4 nm thick[2] and absorbs only 2.3% of incident light.[3] This difficulty was overcome in 2004, when the first graphene sheets were created by mechanical exfoliation of highly ordered graphite and visualized by

immobilizing the sheets on oxidized silicon (Si/SiO_2) wafers. Light interference in the oxide layer (typically 300 nm thick) changes when it is covered by graphene, which allows identification of the graphene on the substrate through color contrast in the reflected light.[2]

The exceptional electrical, optical, and mechanical properties of graphene make it a promising material for many industrial applications, such as solar cells, semiconductor devices, and thermal heat sinks.[4,5] However, the greatest obstacle in its use in industry is high-throughput scaling of the production and characterization of graphene. High-throughput production of graphene can be achieved by growing graphene by chemical vapor deposition (CVD) of carbon atoms on metallic substrates.[6–9] Graphene creation using mechanical exfoliation is labor intensive and only produces a few small graphene samples, whereas the size of CVD-grown graphene is only limited by the size of the growth chamber.[10] CVD-grown graphene has been developed for many different industrial applications, such as electronic devices,[11–13] solar cells,[14,15] and energy storage.[16] The layer thickness and uniformity of a graphene sample are important parameters that affect the performance and properties of the sample. Additionally, cracks and wrinkles in the graphene sample cause variations in the electronic properties that are unrelated to the quality or thickness of the graphene. These defects are difficult to completely avoid due to complicated growth and processing procedures. Therefore, a high-throughput metrology technique that characterizes an entire CVD-grown graphene sample is necessary for industrial applications.

The same obstacle that delayed the discovery of graphene makes high-throughput metrology difficult. Common methods for characterizing graphene thickness are Raman microscopy[17] and atomic force microscopy.[18] While these techniques offer insight into the atomic-scale quality of graphene samples, they are slow and limited to characterizing small regions. To overcome these issues, large-scale optical graphene metrology techniques have been developed that identify the layers of graphene-immobilized Si/SiO_2 substrates based on their color contrast.[6,19] Although Si/SiO_2 substrates offer a simple method for improving the visibility of graphene, they complicate the development of a metrology technique that is suitably robust for industrial use. This is due to the fact that the color sensitivity of cameras changes between camera models and depends on the illumination intensity. Therefore, the color contrast used to identify graphene layers changes between microscopes and slowly changes on the same microscope as the illumination intensity varies. Additionally, the maximum ideal contrast between graphene layers is limited to ≈12%.[20] Therefore, metrology techniques that rely on Si/SiO_2 must be calibrated often, a step that requires Raman spectroscopy to identify each individual graphene layer. Finally, many industrial applications, including solar cells and electronic systems on printed circuit boards, require metrology measurements of graphene samples on substrates other than Si/SiO_2.

Fluorescence quenching microscopy (FQM) offers an alternative to visualizing graphene using Si/SiO_2 substrates and introduces the possibility of high-throughput, large-area metrology of CVD-grown graphene samples on arbitrary substrates. FQM is a novel technique for visualizing graphene that is based on the quenching of fluorescence via resonant energy transfer between dye molecules and graphene.[21–23] FQM is an excellent technique for large-scale graphene metrology because it can be performed on arbitrary substrates, the imaging time is short, large areas can be measured, and the imaging equipment (a fluorescence microscope) is widely available.[24–27] In FQM, the quenching of dye fluorescence is visualized by spin-coating a solution of polymer mixed with a fluorescent dye onto the graphene sample. While graphene quenches dye fluorescence, the substrate does not. Therefore, graphene regions are identified by dark regions in the fluorescence image of the sample. Currently, FQM has been used to visualize small exfoliated graphene and graphene oxide samples but no attempt has been made to achieve quantitative characterization of the graphene samples, such as identifying graphene layers.

Herein, we advance FQM by introducing a method for identifying and counting graphene layers using histogram-based segmentation. Our large-area graphene metrology technique is illustrated in **Figure 1**. Briefly, we coat the graphene sample with a dye–polymer solution and image the sample using a fluorescence microscope. To characterize an entire CVD-grown graphene sample, we collect a large-scale, high-resolution

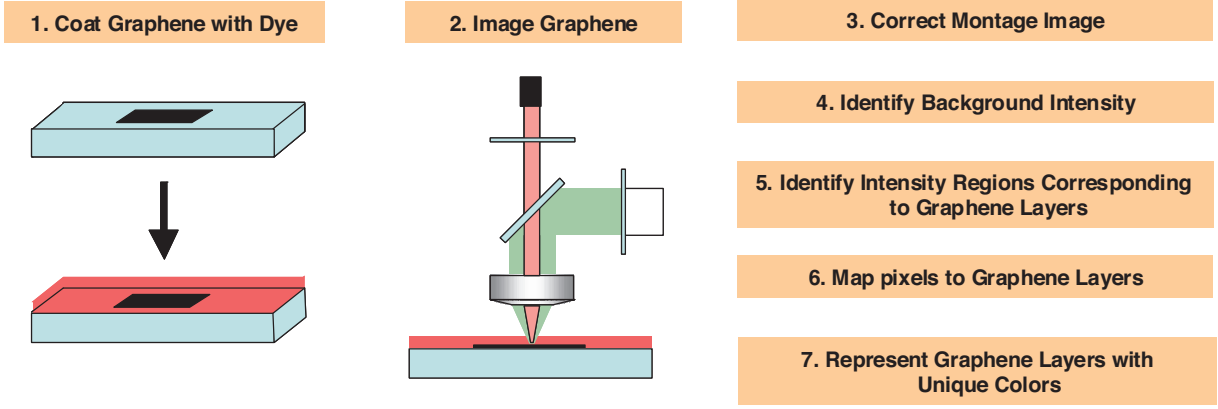

Figure 1. Schematic of the large-area, high-contrast graphene metrology technique.

montage image and process the image to remove the effects of nonuniform illumination. Next, we analyze the histogram of the resulting image to identify the unquenched fluorescence intensity. The intensity ranges within the histogram that correspond to graphene layers are calculated from known contrast ranges relative to the unquenched fluorescence intensity. Finally, the image is segmented by mapping pixels to different graphene layers depending on their intensity values. Utilizing this technique, we achieve high-throughput thickness and uniformity metrology of entire CVD-grown graphene samples on a glass substrate. Because the contrast provided by FQM does not depend on the substrate or sensitivity of the microscope, this method does not require additional calibration, thereby allowing for fully automated metrology measurements. This work introduces a new method for graphene metrology that allows quick and easy identification of CVD-grown graphene layers in a large area on arbitrary substrates.

2. Results and Discussion

2.1. Large-Area High-Contrast Fluorescence Imaging

The contrast between graphene and the substrate can be customized by controlling the thickness of the dye layer, from complete quenching with a dye monolayer[25,28] to negligible quenching with a thick dye layer. In this study, we coated the graphene with a 30-nm-thick dye layer to provide optimal contrast for few-layer graphene. After dyeing the graphene sample, we imaged the graphene with a fluorescence microscope equipped with a mechanical stage. To achieve high-resolution imaging, a 20 × (0.75 numerical aperture, NA) imaging objective was used. With this objective, an image covers a 417 × 318 μm^2 area. To image the entire graphene sample, which covers approximately 1 cm^2, a montage of individual images was collected. This objective can achieve a resolution of 380 nm; however, to reduce the noise in the image and keep the size of the montage image file reasonable, we averaged a 4 × 4 segment of pixels into one final pixel. This resulted in an effective pixel size of 1.24 × 1.24 μm^2. The final image is free from noise and does not need to be further filtered.

The fluorescence montage image of single-layer CVD-grown graphene is shown in **Figure 2**a. The montage consists of 34 × 46 individual images. Because the illumination across one image is not completely uniform, individual images in the montage image can be identified by their dark outlines. This nonuniform illumination can be corrected using the standard microscopy flat-field correction technique. Briefly, a correction image is created by imaging a uniform fluorescence sample such as a dye layer covering a bare substrate. This image should be created using the same imaging pathway used to create the montage image but only needs to be created once every few months as the illumination source ages. Each area in the montage image that represents an individual image is corrected using

$$I_{\text{flat}}(x, y) = \frac{I_{\text{original}}(x, y)}{I_{\text{correction}}(x, y)} \times I_{\text{correction}} \quad (1)$$

The flattened image is shown in Figure 2b. The nonuniform illumination has been entirely corrected. In the flattened FQM image the graphene can be clearly seen and some folds and cracks are apparent.

2.2. Identification of Graphene Layers

Identification of the graphene layers is achieved by histogram-based segmentation based on contrast relative to the substrate. The fluorescence intensity I_f of the dye layer coating the graphene sample is given by

$$I_f = (1 - f_Q) \times I_{f0} \quad (2)$$

where I_{f0} is the original fluorescence intensity of the dye and f_Q is the fluorescence quenching factor, which depends on the number of graphene layers and the thickness of the dye layer. Because the glass substrate does not quench the dye fluorescence, the quenching factor for the substrate is equal to 0 and the fluorescence intensity of the substrate is equal to I_{f0}. Contrast between graphene layers and the background is given by

$$C = \frac{I_{\text{background}} - I_{\text{graphene}}}{I_{\text{background}}} \quad (3)$$

Substituting I_{f0} for $I_{\text{background}}$ and $(1–f_Q)I_{f0}$ for I_{graphene} in Equation (3) gives the relationship between the quenching

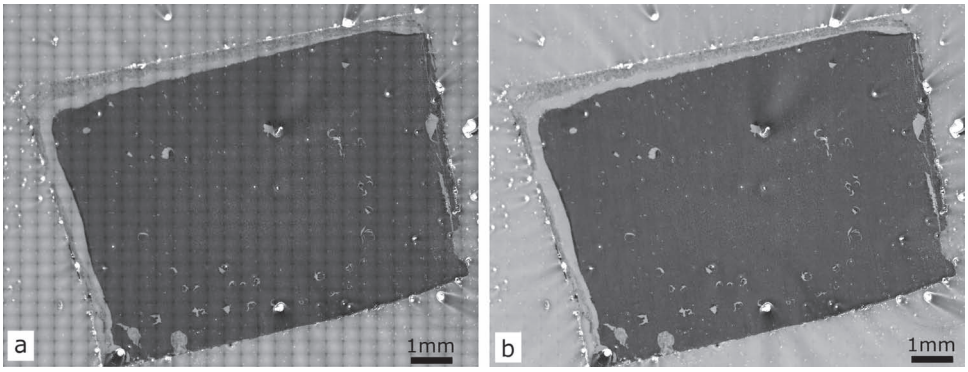

Figure 2. Fluorescence image of dyed CVD-grown graphene sample a) before and b) after background correction.

factor and the contrast between the graphene layer and the substrate

$$C = f_Q \tag{4}$$

The fluorescence intensity of the graphene layers and the substrate can vary between images due to variations in the illumination intensity. However, the contrast between the graphene layers and the substrate is determined by the quenching factor, which is constant across samples and microscopes and depends only on the dye layer thickness.

The first step in our segmentation algorithm is measuring $I_{background}$. This is achieved by analyzing the image histogram. Two major peaks are apparent in the histogram of the corrected fluorescence image of the CVD-grown graphene sample (Figure 2c). The peak at higher fluorescence intensities represents the substrate while the peaks at lower intensities represent the graphene. $I_{background}$ is the intensity value that correlates to the apex of the substrate peak in the histogram. To ensure that the peak corresponding to the substrate is easily identifiable in the image histogram, it is important to design the montage image collection so that the substrate covers a significant portion of the fluorescence image. Once $I_{background}$ is determined, the contrast value for each pixel is calculated according to

$$C(x, y) = \frac{I_{background} - I(x, y)}{I_{background}} \tag{5}$$

Next, the image is segmented according to the pixel contrast value. Our measurements on multiple graphene samples found that for a 30-nm-thick dye layer, the contrast range for single-layer graphene is 0.35–0.58, 0.58–0.75 for two-layer graphene, and 0.75–0.8 for three or more graphene layers. Ideally, the contrast for different layers would be discrete values instead of value ranges. This would be the case for exfoliated graphene samples. CVD-grown samples, however, have variations on the nanometer scale which cannot be adequately resolved due to the diffraction resolution limit of light. The signal from these regions is averaged to obtain the intensity value for each pixel in the collected image. Therefore the intensity peaks in the fluorescence image histogram resemble Gaussian peaks and represent the low-passed version of the ideal discrete peaks.

In addition to identifying graphene layers, our segmentation algorithm identifies contamination on the graphene surface. This is possible because the contamination particles obstruct the distribution of dye as it is spun onto the graphene sample, thus causing the dye to build up around the particles which results in regions where the fluorescence intensity is brighter than the fluorescence of the flat substrate. Similarly, very large contamination blocks the flow of dye, which creates regions with a thinner dye layer. This can lead to incorrect identification of the graphene layers. Therefore, detecting contamination in the segmentation algorithm is important for accurate interpretation of the segmentation results. The contrast range for pixels darker than $I_{background}$ is 0–1 while pixels brighter than $I_{background}$ have negative contrast values. The segmentation algorithm maps pixels to graphene layers, L_n, according to

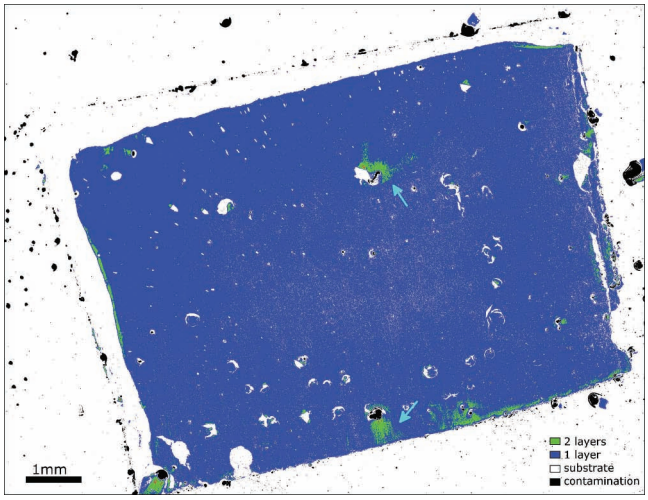

Figure 3. Schematic segmented image of a dyed CVD-grown graphene sample showing different graphene layers and surface contamination.

$$L_n(x, y) = \begin{cases} 3 & 0.75 \le C(x, y) < 0.8 \\ 2 & 0.58 \le C(x, y) < 0.75 \\ 1 & 0.35 \le C(x, y) < 0.58 \\ 0 & -0.2 \le C(x, y) < 0.35 \\ -1 & C(x, y) < -0.2, C(x, y) \ge 0.8 \end{cases} \tag{6}$$

where –1 indicates surface contamination, 0 indicates the substrate, and 3 indicates three or more graphene layers. Applying this segmentation algorithm to the flattened montage fluorescence image in Figure 2b produces the segmented image shown in **Figure 3**. In this image, the graphene layers are portrayed using unique colors. The segmented image shows that the graphene sample is entirely single-layer graphene with some easily identifiable cracks and folds consisting of two-layer graphene. The light blue arrows in Figure 3 indicate regions where large contamination affected the distribution of the dye layer.

To compare the results of our segmentation algorithm with Raman microscopy measurements, we consider a small region from the large-area fluorescence image where the graphene sample exhibits a large crack and a fold. The fluorescence image of this region is shown in **Figure 4**a and the segmented image is shown in Figure 4b. Raman measurements were taken in the areas corresponding to the colored dots in the fluorescence and segmented images. The resulting spectra (Figure 4c) indicate that the graphene sample is mostly single-layer graphene (green dot and spectrum) with two-layer graphene at the fold (blue dot and spectrum) and no graphene in the crack (red dot and spectrum).[17,29–31] In the histogram of the fluorescence image (Figure 4d), intensity ranges mapped to different graphene layers during the segmentation process are indicated. Profiles taken along the lines in the fluorescence and segmented images are compared to the graphene layer thickness measured by Raman microscopy in Figure 4e. Raman microscopy measurements, indicated by the colored dots in the line profile, agree with the layer thickness identified by the segmentation algorithm. Therefore, Raman microscopy confirms that our

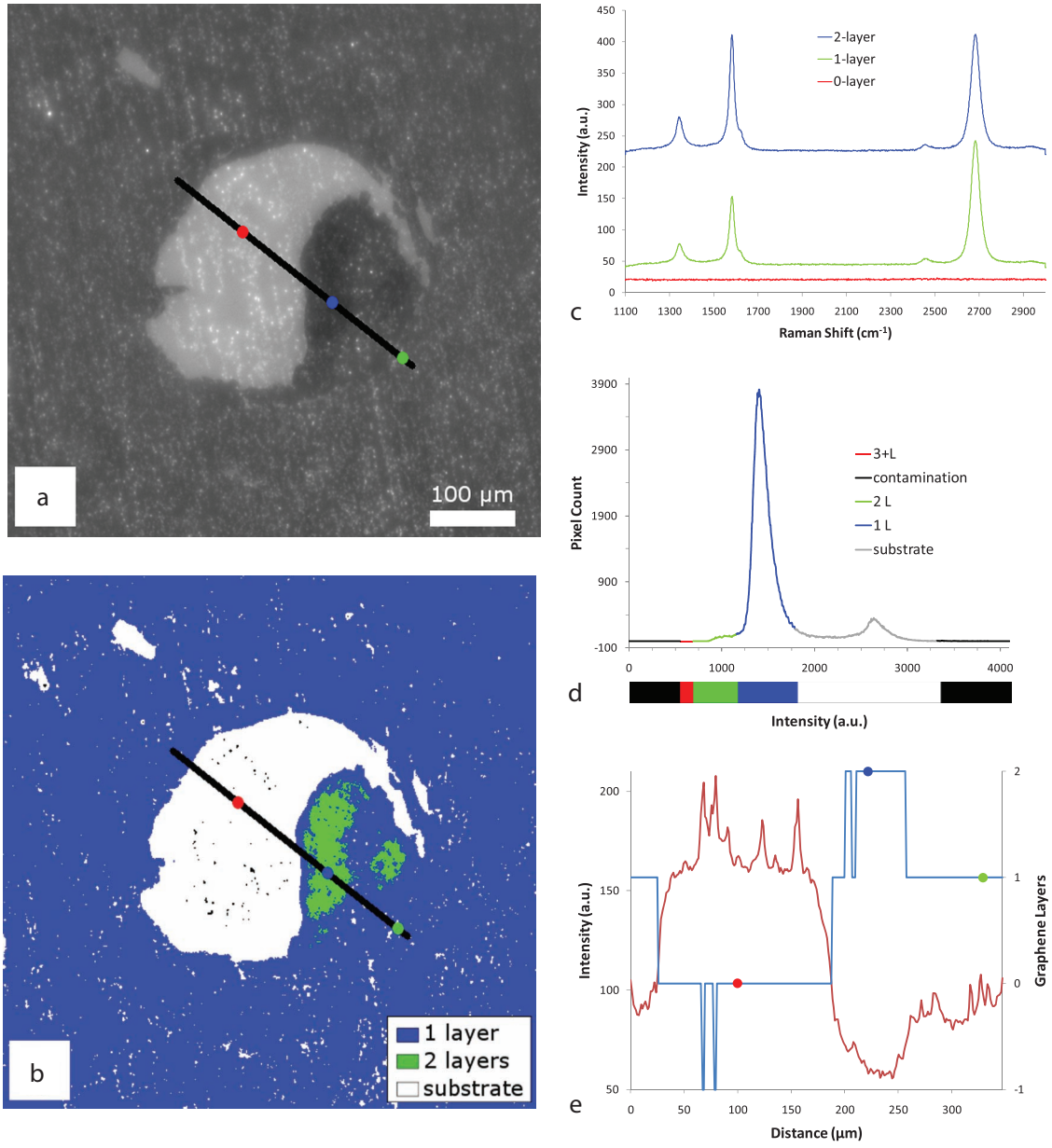

Figure 4. a) FQM and b) segmented images of CVD-grown graphene. c) Raman spectra recorded at colored dots in (a) and (b). Spectra have been offset for visibility. d) Histogram of FQM image. Colored regions indicate intensity ranges mapped to different graphene layers in the segmentation algorithm. e) Line profile from (a) and (b) showing the FQM signal (red line), layer count from segmented image (blue line), and layer count from Raman measurements (colored dots).

segmentation technique accurately measures graphene layer thickness.

2.3. Graphene Layer Quality Comparison

To illustrate the usefulness of this metrology technique for applications such as optimizing graphene growth procedures, we compare the quality of graphene samples prepared using different transfer techniques. An important step in the transfer of graphene is dissolving the cured poly(methyl methacrylate) (PMMA) layer that is used to protect the graphene during the etching and transfer steps. The basic technique is to completely dissolve the PMMA by dipping the entire sample in acetone.[32] Recently it was shown that the quality of the CVD-grown graphene sample is improved when a drop of liquid PMMA is added on top of the transfer PMMA and allowed to slowly dissolve the transfer PMMA for 30 min before the acetone soak.[33] The authors suggested that dissolving the transfer PMMA with liquid PMMA allowed the graphene to relax on the substrate. We propose that similar results can be obtained by adding a drop of acetone instead of liquid PMMA.

The graphene sample shown in Figure 3 was prepared by placing one drop of acetone onto the transfer PMMA and allowing it to dry for 30 min before soaking the sample in

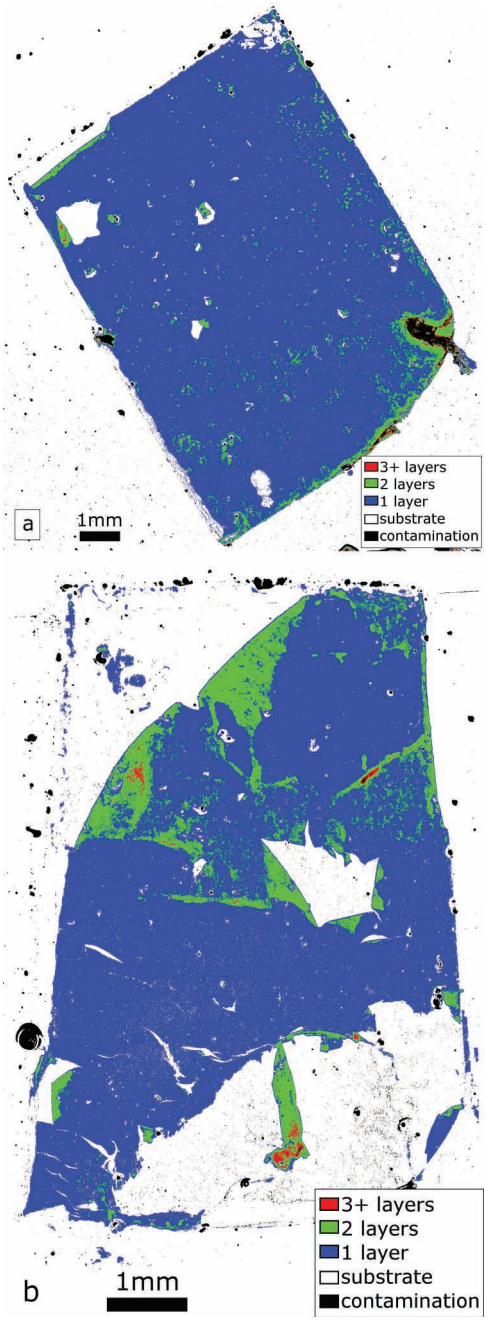

Figure 5. Segmented image of dyed CVD-grown graphene samples prepared using different transfer techniques. a) Modified technique where a drop of liquid PMMA is added to the transfer PMMA and b) unmodified technique where the transfer PMMA is directly dissolved by dipping the sample in acetone.

acetone. For the graphene sample shown in **Figure 5**a, we placed one drop of liquid PMMA onto the transfer PMMA and allowed it to dry for 30 min. As a control, the graphene sample in Figure 5b was prepared by following the unmodified basic transfer technique, in which the sample is directly dipped into acetone to dissolve the PMMA. All three CVD-grown graphene samples were grown on the same copper foil substrate, underwent the same etching process, and were dried overnight after they were immobilized on the glass substrate.

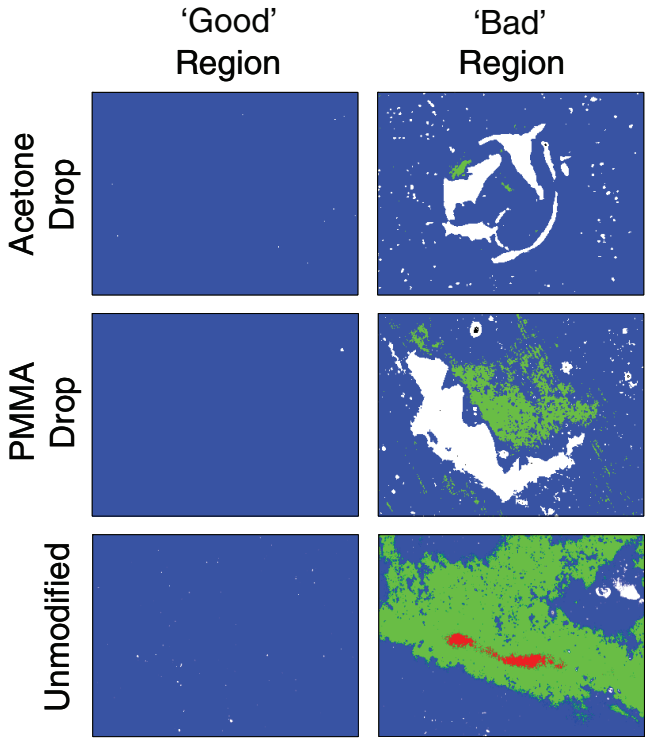

Figure 6. Comparison of different regions in the segmented images of graphene samples. Each region covers a 417 × 318 μm^2 area.

The segmented images of the graphene samples clearly show that the quality of the graphene sample is improved by both the acetone drop and PMMA drop methods. The presence of numerous folds and large cracks in the samples prepared using the unmodified method indicates that the graphene did not adequately relax onto the substrate and was torn when the transfer PMMA was dissolved in the acetone bath. The graphene samples prepared using the acetone drop and PMMA drop methods are of similar quality. Both samples still contain some cracks and folds, thus indicating an opportunity for further improvement of the transfer method.

Figure 6 shows 417 × 318 μm^2 sections of each graphene sample which represent "good" and "bad" regions in the samples. The size of these sections is approximately the size of a single image collected using a 20× objective. Although the large-scale images of the graphene samples show that the modified transfer methods produce graphene samples with improved quality compared to the unmodified transfer method, the small-scale "good" images indicate that the samples are all of equal quality. It is easy to see how a comparison that only uses small-scale images could be comparing "good" regions to "bad" regions in different samples, thereby resulting in incorrect conclusions. Therefore, a large-scale metrology technique is required to accurately compare the quality of CVD-grown graphene samples.

3. Conclusion

In summary, we have introduced a large-scale metrology method for measuring the thickness and uniformity of entire

CVD-grown graphene samples. This method utilizes FQM to increase the contrast between the graphene layers and the substrate and histogram-based segmentation to identify the graphene layers. Unlike methods based on color contrast created using a Si/SiO_2 substrate, this method does not require calibration but is consistent across different samples and microscopes. The contrast range for different graphene layers depends on the dye thickness. In this study, we utilized a dye thickness optimized for few-layer graphene. It is easy to see that this method can be extended to thicker graphene samples by increasing the thickness of the dye layer.

Utilizing the large-scale metrology method described in this work, we have evaluated the effect of different transfer methods on the quality of the resulting CVD-grown graphene layers. We found that adding a drop of acetone to the sample to dissolve the PMMA layer before dipping the sample in acetone yields graphene samples that are of similar quality to samples where a drop of liquid PMMA was added. Both methods improved the quality of the graphene compared to the basic transfer technique, in which the sample is immediately soaked in acetone. Comparison of small-scale images of the different graphene samples revealed that these images do not adequately describe the samples and can lead to incorrect conclusions about the quality of the CVD-grown graphene samples. The large-scale metrology technique described in this work allows for fast and accurate evaluation of the quality of entire CVD-grown graphene samples. The repeatability and flexibility of this technique make it promising for many industrial applications.

4. Experimental Section

Dye-Doped Polymer Preparation and Measurement: The dye mixture was prepared by adding 0.01 wt% 4-(dicyanomethylene)-2-methyl-6-(4-dimethylaminostyryl)-4*H*-pyran (DCM, Sigma–Aldrich) to PMMA (10 mL, 1.0 wt%, $M_w \approx 120\,000$) dissolved in toluene (>99.5%, Fisher Chemical). The low vapor pressure of toluene allowed the formation of extremely uniform dye layers. The solution was stirred and heated overnight to dissolve the polymer, then continuously stirred while stored. Immediately before the solution was spun onto the substrate, it was sonicated for 15 min. To ensure that any bright spots seen in the FQM image of graphene were due to contamination on the surface, the dye solution was passed through a 0.22 µm filter before being deposited on the substrate. The dye layer was formed by flooding the substrate with the dye mixture then spinning the substrate at 3000 rpm for 60 s with a 2 s ramp. Next, the sample was stored in a vacuum desiccator for 1 h to completely evaporate the solvent. This step was necessary to achieve consistent contrast measurements for the graphene layers. As the solvent evaporated, the layer thickness decreased which altered the quenching of the dye layer and the contrast between graphene layers and the substrate. The dye layer thickness was determined by forming scratches in the polymer layer with plastic tweezers and measuring the height difference with a Veeco Dektak 8 surface profilometer. The measured absorption and emission peaks for the dye polymer mixture were 470 and 560 nm, respectively (see Supporting Information).

Graphene Sample Preparation for FQM: Centimeter-scale graphene sheets were grown using a 25-µm-thick copper foil (Alfa Aesar, item No. 13382) as a catalyst.[7] The copper foils were pretreated with acetic acid and deionized (DI) water to ensure the surfaces were completely clean and free from oxidation. Next, the pretreated copper foils were loaded into a quartz-tube furnace chamber, heated to 1000 °C in a 2 Torr Ar/H_2 (200:200 sccm) atmosphere, and thermally annealed for 30 min. For the growth of graphene, methane (100 sccm) was introduced into the chamber under 20 Torr for 20 min and the chamber temperature was reduced to 25 °C at a cooling rate of 20 °C min^{-1}. The graphene samples were removed from the growth chamber, covered with PMMA by drop-coating, and heated at 120 °C for 10 min to dry the PMMA layer. The copper foil was then etched in iron(III) chloride ($FeCl_3$) aqueous solution (0.5 M) and rinsed thoroughly with hydrochloric acid (3%) and DI water.

Glass substrates were prepared by cutting microscope slides into 1 in^2 squares and cleaning by gently rubbing with a clean gloved finger and liquid detergent, followed by sonication for 10 min each in DI water, toluene, acetone, and isopropyl alcohol (IPA) and finally blowing dry with a nitrogen stream. Floating graphene samples were fished onto the substrate and allowed to dry overnight. To remove the transfer PMMA from the graphene, the samples were soaked in heated acetone for 30 min, soaked in heated IPA for 10 min, and dried under a nitrogen stream. The samples were stored in a vacuum desiccator.

Image Acquisition: Fluorescence images of the dye-coated graphene were collected using a BD Pathway 855 HT confocal microscope. An arc lamp was used as the light source. The illumination light was filtered through a 470 nm (±40 nm) bandpass filter and a dichroic filter (520 nm) and focused on the sample using an Olympus 20× objective with a 0.75 NA. The emitted light was passed through a 542 nm (±27 nm) bandpass filter and detected with a CCD camera. BD AttoVision software, which is provided with the Pathway microscope, was used to control the mechanical stage and collect montage images.

Image Processing: All image processing was performed on a standard laptop using Matlab software.

Supporting Information

Supporting Information is available from the Wiley Online Library or from the author.

Acknowledgements

We gratefully acknowledge funding for this work by the CMMI Division of the National Science Foundation (Award: 0800680), the Materials Research Science and Engineering Center (NSF-MRSEC) on Polymers (Award: 0213695), the Nanoscale Science and Engineering Center (NSF-NSEC) on Hierarchical Manufacturing (CHM, Award: 0531171), and the Riverside Public Utilities. We would also like to thank Dr. David Carter from the Center for Plant Cell Biology at the University of California Riverside for helpful discussions on fluorescence imaging.

[1] A. Cho, *Science* **2010**, *330*, 159.
[2] K. Novoselov, A. Geim, S. Morozov, D. Jiang, Y. Zhang, S. Dubonos, I. Grigorieva, A. Firsov, *Science* **2004**, *306*, 666.
[3] R. R. Nair, P. Blake, A. N. Grigorenko, K. S. Novoselov, T. J. Booth, T. Stauber, N. M. R. Peres, A. K. Geim, *Science* **2008**, *320*, 1308.
[4] A. Castro Neto, F. Guinea, N. Peres, K. Novoselov, A. Geim, *Rev. Mod. Phys.* **2009**, *81*, 109.
[5] A. Geim, K. Novoselov, *Nat. Mater.* **2007**, *6*, 183.
[6] A. Reina, S. Thiele, X. Jia, S. Bhaviripudi, M. Dresselhaus, J. Schaefer, J. Kong, *Nano Res.* **2009**, *2*, 509.
[7] X. Li, W. Cai, J. An, S. Kim, J. Nah, D. Yang, R. Piner, A. Velamakanni, I. Jung, E. Tutuc, S. K. Banerjee, L. Colombo, R. S. Ruoff, *Science* **2009**, *324*, 1312.
[8] A. N. Obraztsov, *Nat. Nanotechnol.* **2009**, *4*, 212.
[9] A. Reina, X. Jia, J. Ho, D. Nezich, H. Son, V. Bulovic, M. S. Dresselhaus, J. Kong, *Nano Lett.* **2009**, *9*, 30.
[10] M. Allen, V. Tung, R. Kaner, *Chem. Rev.* **2010**, *110*, 132.
[11] Z. Chen, Y. Lin, M. Rooks, P. Avouris, *Physica E* **2007**, *40*, 228.
[12] J. Lin, D. Teweldebrhan, K. Ashraf, G. Liu, X. Jing, Z. Yan, R. Li, M. Ozkan, R. K. Lake, A. A. Balandin, C. S. Ozkan, *Small* **2010**, *6*, 1150.
[13] X. Wang, Y. Ouyang, X. Li, H. Wang, J. Guo, H. Dai, *Phys. Rev. Lett.* **2008**, *100*, 206803.
[14] L. De Arco, Y. Zhang, C. Schlenker, K. Ryu, M. Thompson, C. Zhou, *ACS Nano* **2010**, *4*, 2865.
[15] J. Lin, M. Penchev, G. Wang, R. K. Paul, J. Zhong, X. Jing, M. Ozkan, C. S. Ozkan, *Small* **2010**, *6*, 2448.
[16] R. Paul, M. Ghazinejad, M. Penchev, J. Lin, M. Ozkan, C. Ozkan, *Small* **2010**, *6*, 2309.
[17] A. C. Ferrari, J. C. Meyer, V. Scardaci, C. Casiraghi, M. Lazzeri, F. Mauri, S. Piscanec, D. Jiang, K. S. Novoselov, S. Roth, A. K. Geim, *Phys. Rev. Lett.* **2006**, *97*, 187401.
[18] S. Stankovich, D. A. Dikin, G. H. B. Dommett, K. M. Kohlhaas, E. J. Zimney, E. A. Stach, R. D. Piner, S. T. Nguyen, R. S. Ruoff, *Nature* **2006**, *442*, 282.
[19] C. M. Nolen, G. Denina, D. Teweldebrhan, B. Bhanu, A. A. Balandin, *ACS Nano* **2011**, DOI 10.1021/nn102107b.
[20] P. Blake, E. W. Hill, A. H. Castro Neto, K. S. Novoselov, D. Jiang, R. Yang, T. J. Booth, A. K. Geim, *App. Phys. Lett.* **2007**, *91*, 063124.
[21] R. S. Swathi, K. L. Sebastian, *J. Chem. Phys.* **2008**, *129*, 054703.
[22] R. Swathi, K. Sebastian, *J. Chem. Phys.* **2009**, *130*, 3077292.
[23] R. Swathi, K. Sebastian, *J. Chem. Sci.* **2009**, *121*, 777.
[24] J. Kim, L. Cote, F. Kim, J. Huang, *J. Am. Chem. Soc.* **2010**, *132*, 260.
[25] E. Treossi, M. Melucci, A. Liscio, M. Gazzano, P. Samori, V. Palermo, *J. Am. Chem. Soc.* **2009**, *131*, 15576.
[26] A. Sagar, K. Kern, K. Balasubramanian, *Nanotechnology* **2010**, *21*, 015303.
[27] J. Kim, F. Kim, J. Huang, *Mater. Today* **2010**, *13*, 28.
[28] L. Xie, X. Ling, Y. Fang, J. Zhang, Z. Liu, *J. Am. Chem. Soc.* **2009**, *131*, 9890.
[29] I. Calizo, W. Bao, F. Miao, C. Lau, A. Balandin, *Appl. Phys. Lett.* **2007**, *91*, 201904.
[30] H. Cao, Q. Yu, R. Colby, D. Pandey, C. Park, J. Lian, D. Zemlyanov, I. Childres, V. Drachev, E. Stach, M. Hussain, H. Li, S. Pei, Y. Chen, *J. Appl. Phys.* **2010**, *107*, 044310.
[31] Y. Wang, Z. Ni, T. Yu, Z. Shen, H. Wang, Y. Wu, W. Chen, A. Wee, *J. Phys. Chem. C* **2008**, *112*, 10637.
[32] A. Reina, H. Son, L. Jiao, B. Fan, M. Dresselhaus, Z. Liu, J. Kong, *J. Phys. Chem. C* **2008**, *112*, 17741.
[33] X. Li, Y. Zhu, W. Cai, M. Borysiak, B. Han, D. Chen, R. D. Piner, L. Colombo, R. S. Ruoff, *Nano Lett.* **2009**, *9*, 4359.

Received: February 6, 2011
Published online:

